Air Quality Modelling Methodology

1. Air Quality Modeling Tool: PATH-2016

A working group composed of local academics and relevant staff of the Environmental Protection Department (EPD) has been formed to review the adequacy and robustness of EPD's air quality modelling approach and air quality modelling tools for Environmental Impact Assessments (EIAs). The updated PATH-2016 model system has accepted that is capable of accounting for the changes to future air quality resulting from technology changes and deliberate government policies to improve air quality, both in Hong Kong and the surrounding areas, if the emission input to PATH-2016 is properly represented.

The PATH-2016 system consists of three major modules: a meteorological driver, an emission module and a chemical transport model. These are supported by the corresponding input data (see schematics in Figure 1).

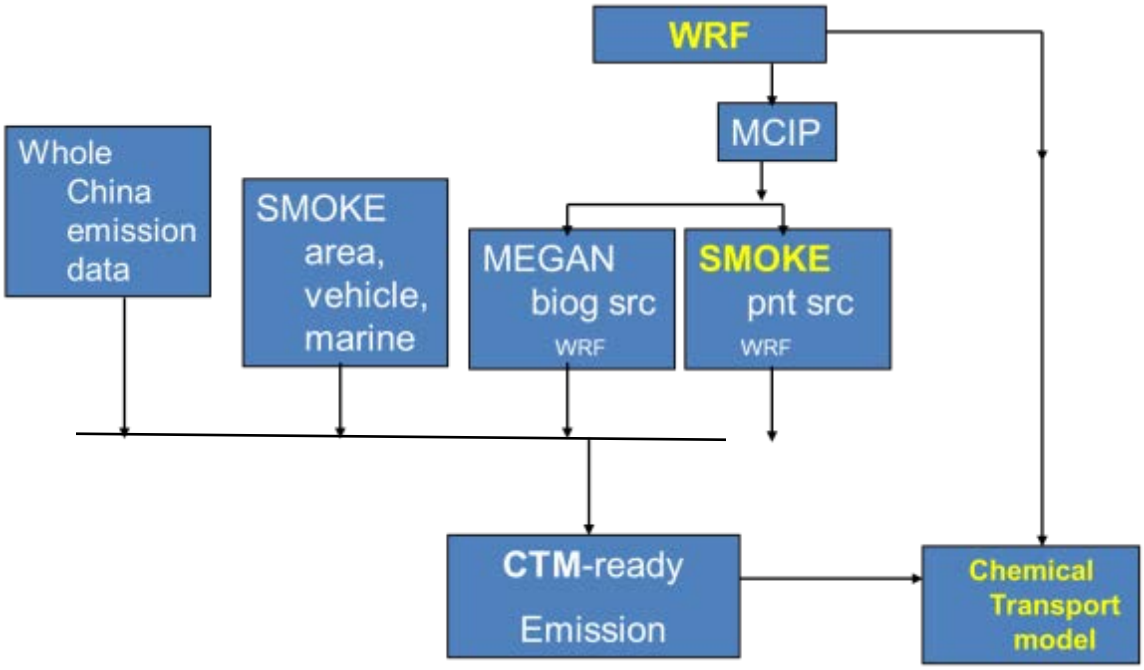

Figure 1. Schematics of the PATH-2016 system.

PATH-2016 is set up on a three-dimensional grid system with 4 horizontal nested domains. Four nested meshes with grid spacing of 27, 9, 3 and 1 km are used for the modeling domains of the meteorological and Chemical Transport Model (CTM). The characteristics of the current configuration are as follows:

Grid 1 (27 km): The coarsest outer grid would include almost all of China and Japan as well as Taiwan, Vietnam, Laos, Cambodia, Thailand, etc.

Grid 2 (9 km): The second grid would cover Southeastern China including Guangdong Province, Hong Kong and Macau.

Grid 3 (3 km): The third nested grid covers most of Guangdong Province, Hong Kong and Macau.

Grid 4 (1 km): The fourth grid is focused on the PRD region.

Figure 2 shows the horizontal extents of the four modeling domains (referred as D1, D2, D3, and D4). The domains of the CTM is slightly smaller and are nested in the meteorological model domain. All of the modeling domain configurations employ a common Lambert-Conformal map projection coordinate system using the map projection parameters listed in Table 1. Table 2 summarizes the domain configuration for the WRF model applications.

The largest domain (D1) shown in Fig. 2a is designed so that the Pearl River Region (PRD) is located at the central longitude of D1. The east-west dimension of D1 is extended so that the abruptly elevated Tibetan Plateau is included in the domain and is not cut by the eastern boundary of D1. It is well known that numerical instabilities may be generated if the model domain boundary cuts the Tibetan Plateau and so a smaller time step should be chosen to run the model to alleviate this problem and this results in a longer running time.

The vertical atmosphere is resolved to 38 layers, with thinner layers in the planetary boundary layer. The layer configuration is selected to capture the important diurnal variations in the boundary layer while also to have layers in the upper troposphere to try and resolve convective activity. The vertical structure of the models is primarily defined by the vertical grid used in the WRF modeling. The WRF model employs a terrain following coordinate system (so-called sigma coordinate system) defined by the pressure levels at surface and top (usually using the standard values of 1000 and 50 hPa respectively). The vertical grid of the meteorological models use 38 vertical layers that extend from the surface to the 50 hPa pressure level (approximately 23 km height). More than half of the vertical levels (about 20) are situated at the lower troposphere (below approximately 1750 m height) within the Planetary Boundary Layer (PBL) where most of the atmospheric processes occur that lead to elevated pollution levels in the HK and PRD regions. Now we have 19 layers from 0m to 1,500m, 11 layers from 1,500m to 8,000m, and 8 layers from 8,000 m to 20,000m. The thickness of the first model layer is taken to be 17m.

(a)

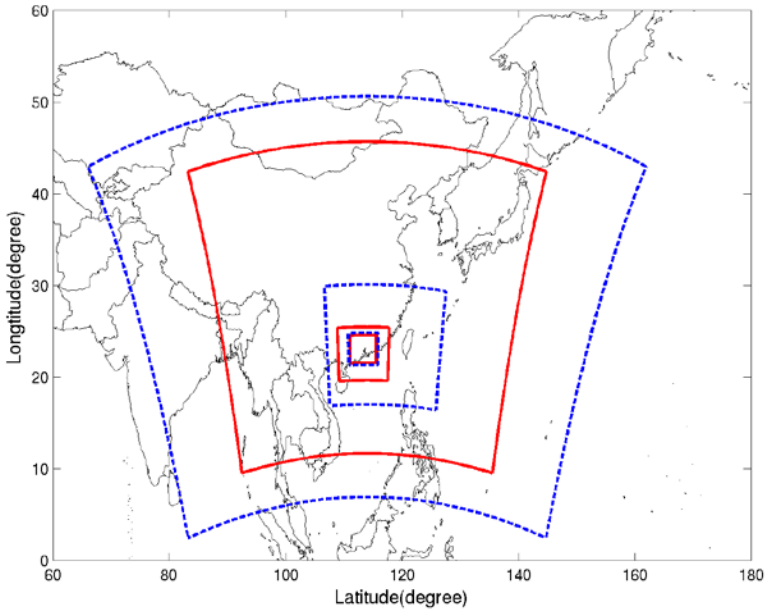

(b)

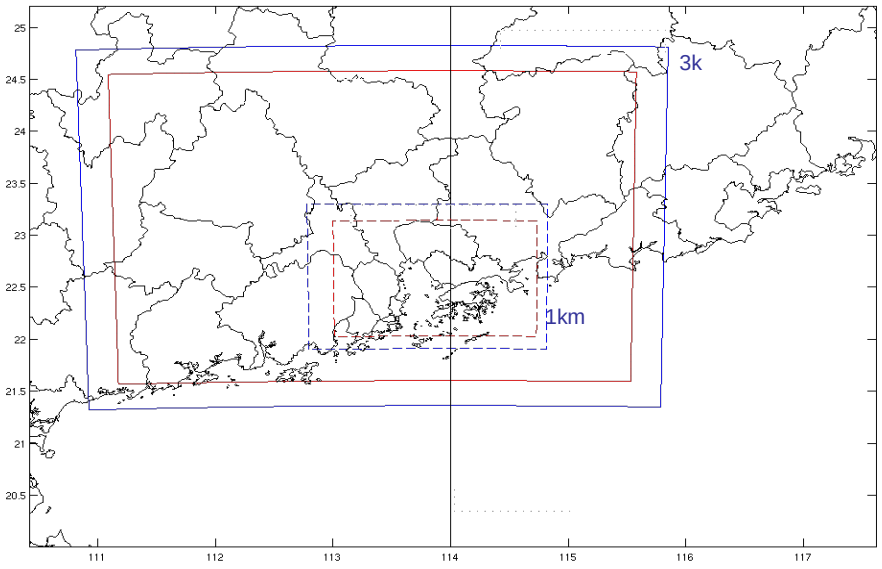

Figure 2a shows D1 and D2 domains. WRF domains are represented by blue and the CTM domains are represented by red.

Figure 2b shows D3 and D4 domains. WRF domains are represented by blue and the CTM domains are represented by red.

Table 1 PATH-2016 coordinate system projection parameters.	
Parameter	**Value**
projection	Lambert-Conformal
alpha (true latitude 1)	15 degrees North Latitude
beta (true latitude 2)	40 degrees North Latitude
x center	114 degrees East Longitude
y center	28.5 degrees North Latitude

Table 2 PATH-2016 grid configuration for the WRF model application.				
Domains	**D1**	**D2**	**D3**	**D4**
Gird Sizes (km)	27	9	3	1
Grid points in Y-direction	184	163	130	163
Grid points in X-direction	283	223	172	214
Lower left Y in parent domain	1	45	55	22
Lower left X in parent domain	1	116	43	67

The thickness of the first model layer is taken to be 17 m. The relevant outputs of the PATH-2016 systems are: gridded meteorological and pollutant concentration data every hour of the simulation period.

Note that EPD has made available model outputs for public access (http://www.epd.gov.hk/epd/english/environmentinhk/air/guide_ref/guide_aqa_model.html). These include:

- Meteorological data for one representative year appropriate to drive air quality simulations using PATH-2016, and
- Hourly concentrations over the first ten layers of the PATH-2016 domain for NO, NO_2, SO_2, RSP, O_3 and CO for some future years. These concentrations are linearly interpolated between model outputs for at least 2 years which are generated using EPD's best estimate / projection of emissions and the meteorological data for the representative year.

2. Assessment/Model Year

2.1 Base year 1 – 2015

We will use the latest emission inventory (2015) for HK from HKEPD as a base year. The other emission inventory (PRD-2012) will be provided from Prof. Allen Zheng of SCUT. An anthropogenic emission inventory (MIX-2010) for outer domains (D1, D2 and part of D3) is provided from Tsinghua University. Emissions are estimated for all major anthropogenic sources in 30 countries and regions in Asia. The resolution of MIX is 0.25 degree by 0.25 degree resolution.

2.2 Base year 2 – 2020

This emission inventory will be provided by HKEPD. The purpose of this study is to access whether the state of the air quality in 2020 will meet the current AQO standard or not.

2.3 Target year – 2025

This emission inventory will be obtained by projecting various air quality improvement measures by the study groups (road transportation, marine transportation, and energy and power generation) as well as known control strategies taken in China. The purpose of this study is to evaluate the air quality improvement in 2025, against the results of the baseline scenarios for years 2015 and 2020 provided by HKEPD. This study will also compare the air quality assessment results under different control scenarios with WHO AQGs and ITs and propose optimum scopes for tightening the AQO.

3. Meteorological Input

To run the meteorological models, some basic input data are required. The data can be classified into two categories, those required for model setup and operation, and those required for initial and boundary conditions to run the model. Below are the basic input data for the meteorological models. The model period is for the whole year of 2015.

3.1 Topographic Data

Terrain elevation data are obtained from the National Center for Atmospheric Research (NCAR) and the U.S. Geological Survey (USGS) terrain databases. The data are available at six resolutions from the USGS: 1-degree, 30-, 10-, 5-, 2-minutes and 30-second. All lower resolution data (1 degree to 2 minutes) are created from the 30 seconds USGS data. Terrain data will be interpolated to the model grid using the TERRAIN pre-processor. The WRF model uses terrain data with resolutions from 10 minutes to 30 seconds according to the grid sizes of the model domains.

3.2 Vegetation Type and Landuse Data

Global 24-category vegetation type and landuse data obtained from the NCAR and USGS databases are used. The data comprises global coverage with the resolution of 1-degree, 30-, 10-, 5-, 2-minutes and 30-seconds (all lower resolution data are created from 30 sec data from USGS version 2 land cover data). The WRF model uses terrain data with resolutions from 10 minutes to 30 seconds according to the grid sizes of the model domains.

Some previous studies (e.g. Lo et al. 2006, 2007; Yim et al. 2007) have indicated that the regional circulation and land-sea breeze system in the Pearl River Delta (PRD) region can be better simulated if a more realistic landuse is used for the region. As suggested by these studies, in the PATH meteorological models, an updated landuse (year 2012) over the PRD has been used to replace the outdated (year 1993) one from the USGS which was derived from 1-km Advanced Very High Resolution Radiometer (AVHRR) data in a 12-month period spanning from April 1992 to March 1993. As shown in Figure 3, the main difference between the new and the old landuse data is that urban areas in the PRD region have substantially increased. Much larger urban areas (yellow color) (increased by a factor of about 25) have developed in the PRD region since 1993. In 1993, only 0.9% of the land area was classified as urban. Most of the land area was cropland. By 2012, the urban area has increased to about 22.2% of the total land area. With this rate of urbanization, local meteorological conditions including land-sea breezes and heat island effects have changed markedly (Fung et al. 2005, Lam et al. 2006 and Lo et al. 2006).

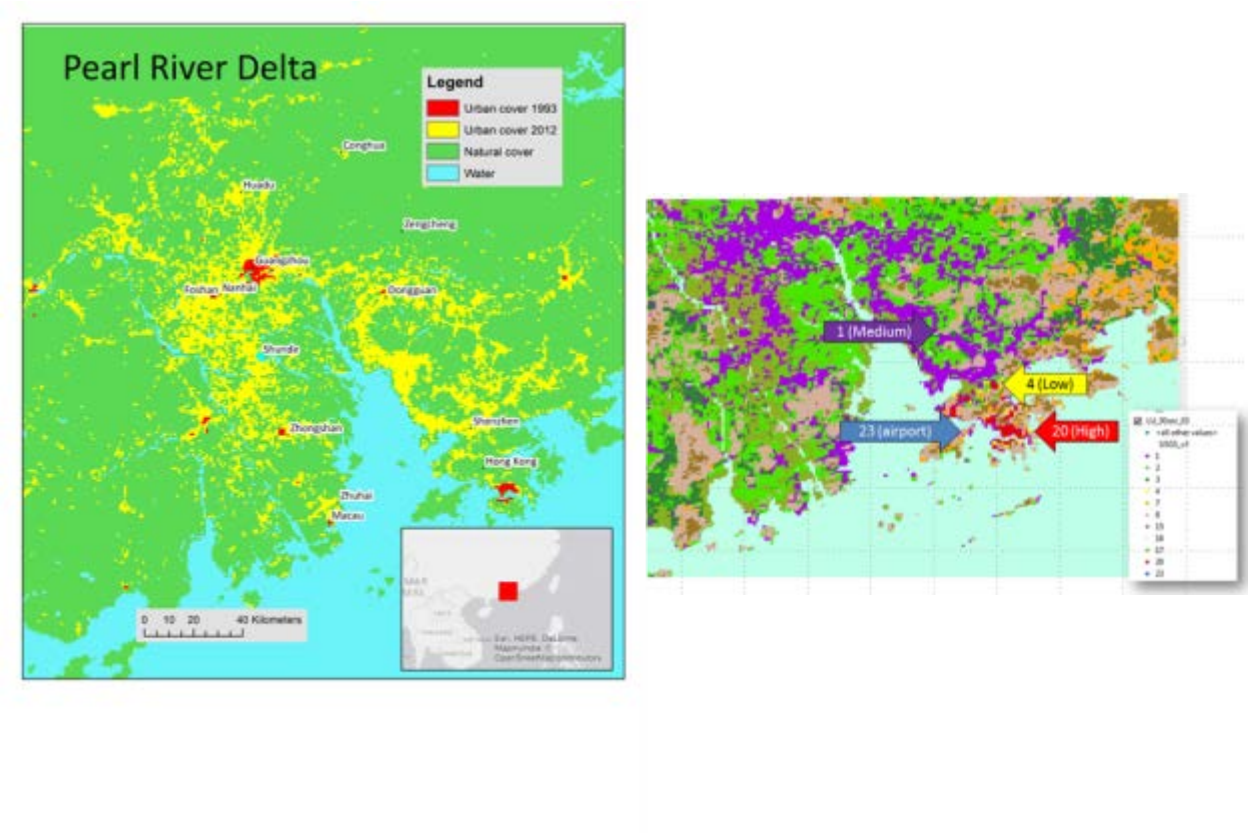

Fig 3 shows the updated landuse of the PRD region.

3.3 Atmospheric Data

Initial conditions, lateral boundary conditions and Four-Dimensional Data Assimilation (FDDA) three-dimensional grid nudging fields are based on the Final Analysis (FNL) data obtained from the National Centers for Environmental Prediction (NCEP).

The NCEP analysis are chosen as initial and boundary conditions mainly because of their availability for download through the internet in near real-time (within a few hours after the model forecasts is started). The resolution of the NCEP data is 1-degree. The NCEP collects observations for at least 6 hours past synoptic time and makes a global analysis and 3, 6, and 9 hour forecasts 4 times per day. The FNL data are suitable for running historical cases. The WRF runs are initialized using $1^{o}x1^{o}$ NCEP Final Analysis data as a first guess field. Observations available on the Global Telecommunication System (GTS) are incorporated in WRF initial conditions through the program OBSGRID. The “skin temperature” field in the FNL and GFS data are used for sea surface temperature inputs.

3.4 Data Assimilations

The four-dimensional data assimilation (FDDA) scheme included in WRF is based on Newtonian relaxation or "nudging". Nudging is a continuous form of FDDA where artificial (non-physical) forcing functions are added to the model's prognostic equations to nudge the solutions toward either a verifying analysis or toward observations. The artificial forcing terms are scaled by a nudging coefficient that is selected so that the nudging term will not dominate the prognostic equations. The nudging terms tend to be one order of magnitude smaller than the dominant terms in the prognostic equations and represent the inverse of the e-folding time of the phenomena captured by the observations.

There are two types of nudging in WRF: analysis nudging and observation nudging ("obs. nudging"). Analysis nudging gently forces the model solution toward gridded fields. Analysis nudging can make use of three-dimensional analyses and some surface analyses. Analysis nudging is generally used for scales where synoptic and meso-alpha forcing are dominant. Obs. nudging gently forces the model solution toward individual observations, with the influence of the observations spread in space and time. Obs. nudging is better suited for assimilating high frequency, a synoptic data that may not otherwise be included in an analysis.

Nudging in WRF is extensively discussed in Stauffer and Seaman (1994) and Seaman et al. (1995). The data assimilation is generally used throughout the MM5/WRF simulation period for air quality simulations. Three-dimensional analyses of wind, temperature, and moisture are assimilated, and only surface analyses of wind are assimilated, following Stauffer et al. (1994).

Surface wind data from automatic weather stations (more than 700) provided by the Hong Kong Observatory and China are used for the observational nudging of the surface wind field in D4. Observational nudging of the thermodynamic variables are not performed.

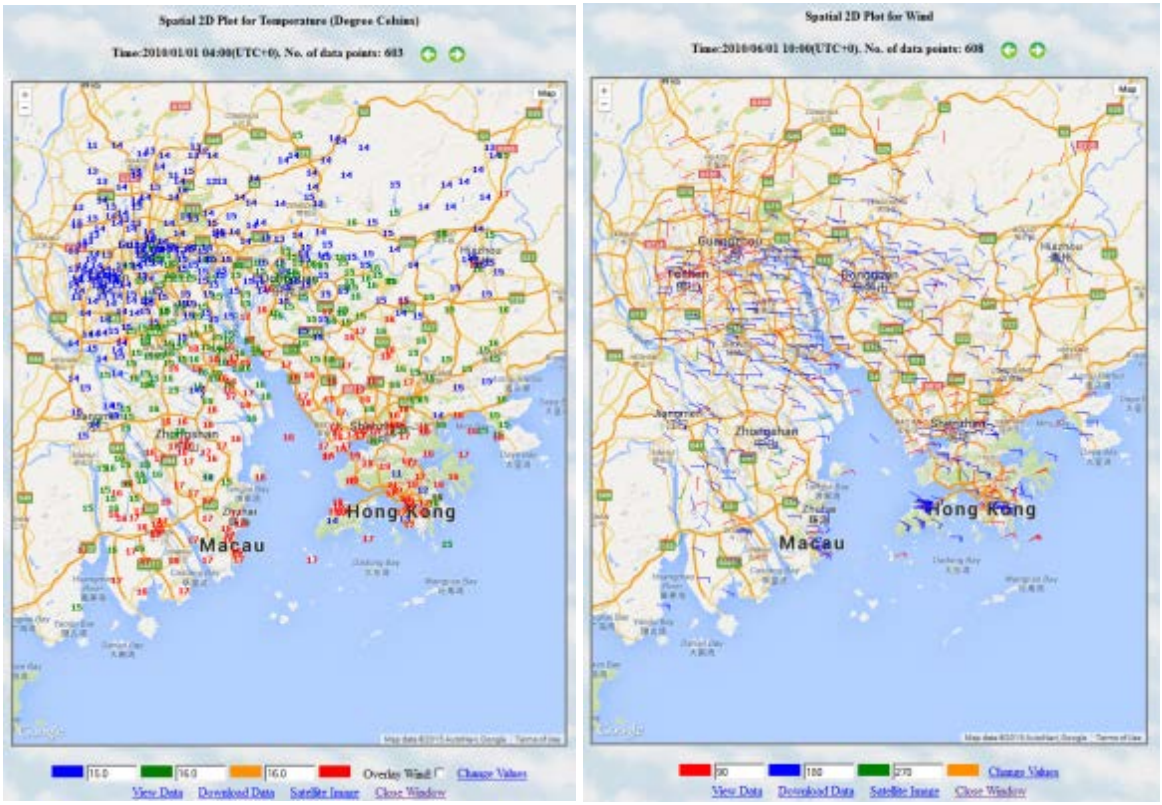

Figure 4 shows the spatial distribution of AWS stations used for data assimilations.

3.5 Meteorological Model Validations

The simulated meteorological field of 2015 has already completed as provided by EPD, Appendix A shows some sample plots of wind and temperature comparisons between simulation results and observations at some meteorological stations between Jan 1 – March 31, 2015 as well as some annual model performance statistics. The results demonstrated that the simulated wind field is good and can be used for driving the Community Multi-scale Air Quality (CMAQ) modelling system for different control scenario studies.

4. Emission Input

Emissions data are processed in two separate approaches, based on availability for D4 and D3, with resolution of 1 and 3 km, annual emission amounts of 2015 for Hong Kong will be provided by the HKEPD; while annual emission amounts for the PRD have been updated to year 2012 by Professor Allen Zheng from SCUT. A bottom-up approach was adopted for power plant and industrial sources to 8 cities within the PRD economic zone, while a top-down approach has been used for area sources and other emission categories. Emissions from marine vessels and shipping lines will be updated in this study. Vessel track data from the Automatic Identification System (AIS) and World registered ships database are utilized to obtain marine vessel activity data. Activity-based approach is used to develop the marine vessel emission inventory in Southern China, Pearl River Delta and in Hong Kong. The spatial distribution of marine emission will be estimated on a 500 m resolution spatial grid to investigate emission situation and assisted in decision making on control policy or regulations.

The Sparse Matrix Operator Kernel Emissions (SMOKE version3.7; http://www.smoke-model.org/) modeling system was used to distribute the total emission amount using WRF outputs and geographic information in time-varying gridded emission files which are served as emission input files for air quality model CMAQ.

4.1 SMOKE

The emission processing system to be used for air quality forecasting/modelling is SMOKE3.7 which is a very new released version using sparse matrix approach that can permit rapid and flexible processing of emission data.

Emissions modelling is a very complex and difficult process. It requires the wide range of knowledge and experience to process emission inventories into data that can be used by air quality models (AQMs). The emission processing system requires meteorological inputs, an emission inventory, and other ancillary input files to do temporal allocation, spatial allocation and chemical speciation (see also Appendix B for some sample plots). During this process, SMOKE creates matrices of speciation factors, gridding factors, control factors and a vector of hourly emissions. These are then multiplied together to create model ready input data. An emission processing system requires both meteorologically dependent inputs such as wind and temperature.

4.2 Emission inventory in 4 domains for base year 1 - 2015

Emissions data are processed in three separate approaches including Hong Kong (HK) region Guangdong (GD) region and outside GD area (remaining regions excluding GD and HK within targeted domains) based on availability of data. Annual emission amounts of 2015 for Hong Kong, will be provided by the HKEPD while total amounts for GD have been updated to year 2012 based on Yin et al. (2015), Zheng et al. (2009). A bottom-up approach was adopted for different sources to all the cities within the Guangdong province. The MIX emission inventory conducted in 2015 was applied for D1 and D2 (Li et al., 2015). In addition, regions in D3 but outside the PRD economic zone are also adopted from the MIX emission inventory.

For biogenic emissions, emission factors from satellite information are used in the MEGAN (Model of Emissions of Gases and Aerosols from Nature) (Guenther et al., 2006) to allocated isoprene, monoterpene and other biogenic volatile organic compounds (BVOCs). Other than emission file and meteorological data, boundary condition (BCON) and initial condition (ICON) are needed to drive CMAQ for each domain. For the outermost domain (D1) of this study, BCON and ICON are extracted from the global model GEOS-Chem outputs (Fu et al. 2008) in order to meet the background concentration in Asian regions. Except for the outer most domains (D1), BCON and ICON for the nested domains are obtained from mother domains. For example, BCON and ICON for D2 is extracted from D1 output file, so does D3 and D4.

With emissions and meteorology inputs in hand, we are ready to use the air quality model CMAQ for CTM simulation. In this study, the Piecewise Parabolic Method (PPM) advection scheme is selected as horizontal diffusion, while K-theory is selected for vertical diffusion. CB05 is used as gas-phase chemistry mechanism, ISORROPIA (a thermodynamic equilibrium model for the K+–Ca2+–Mg2+–NH4+–Na+–SO42−–NO3−–Cl−–H2O aerosol system) for inorganic gas/aerosol partitioning, SOAP for Secondary Organic gas/Aerosol Partitioning, and Regional Acid Deposition Model (RADM) algorithm for aqueous-phase chemistry. Chemistry solver is the Euler-Backward Iterative (EBI). Initial/boundary conditions for the outermost domain of this study originate from the global model GEOS-Chem outputs (Fu et al., 2008) to meet the background concentration in Asian regions.

4.3 Emission inventory in 4 domains for base year 2 - 2020

Projecting the emission inventory in this model year:

HK emission inventory of 2020 will be provided by HKEPD.

PRD emission inventory will be projected base on the Guangdong 13th Five-Year Plan for Environmental Protection which is from 2016 to 2020. The projection is shown in Table 1. All the primary pollutants will be uniformly reduced by certain percentage amount as proposed in the 13th Five-Year Plan.

- After implementation of policies and control measures, at the year 2020, it is expected:
  - ✓ Major air pollutants concentration gradually decrease
  - ✓ Control the Ozone pollution within Pearl River Delta Region

"Thirteen Five" Class B Objective	Year 2015	Year 2020
Days with good air quality per year (%)	91.5	92.5
Yearly Average $PM_{2.5}$ Concentration ($\mu g/m^3$)	34	Less than 33
Yearly Average $PM_{2.5}$ Concentration within unqualified cities in Guangdong Province ($\mu g/m^3$)	39	Less than 35
CO standard compliance cities within Guangdong (%)	-	100
SO_2 total emission amount reduction (%)	-	3
NO_x total emission amount reduction (%)	-	3
VOC total emission amount reduction (%)	-	18
Industrial Smoke/Dust total emission amount reduction	-	15

Regions	Maximum Yearly Average $PM_{2.5}$ Concentration ($\mu g/m^3$)	
	Year 2015	Year 2020
Pearl River Delta Region	40	Less than 35
Guangdong Province East Regions	39	Less than 35
Guangdong Province West Regions	32	Less than 32
Guangdong Province North Regions	35	Less than 35

Table 1. Indicators for environmental protection in the 13th Five-Year Plan in PRD

For D1 and D2, the projection of China emissions shall consider the emission reduction targets proposed in China's 13th 5-year plan (2016-2020) or no change as in 2015.

4.4 Emission inventory in 4 domains for target year - 2025

Projecting the emission inventory in this model year:

HK emission inventory of 2025 will be obtained by projecting various air quality improvement measures by the study groups (road transportation, marine transportation, and energy and power generation) as well as known control strategies taken in Hong Kong.

PRD emission inventory will be projected based on the announced targets by the Guangzhou Environmental Protection Bureau (EPB) (Liu et al. 2013). Figure 5 below provides total estimated emission amounts from each category in 2010 and 2025. Both primary PM2.5 emission and other precursors' emissions would be reduced.

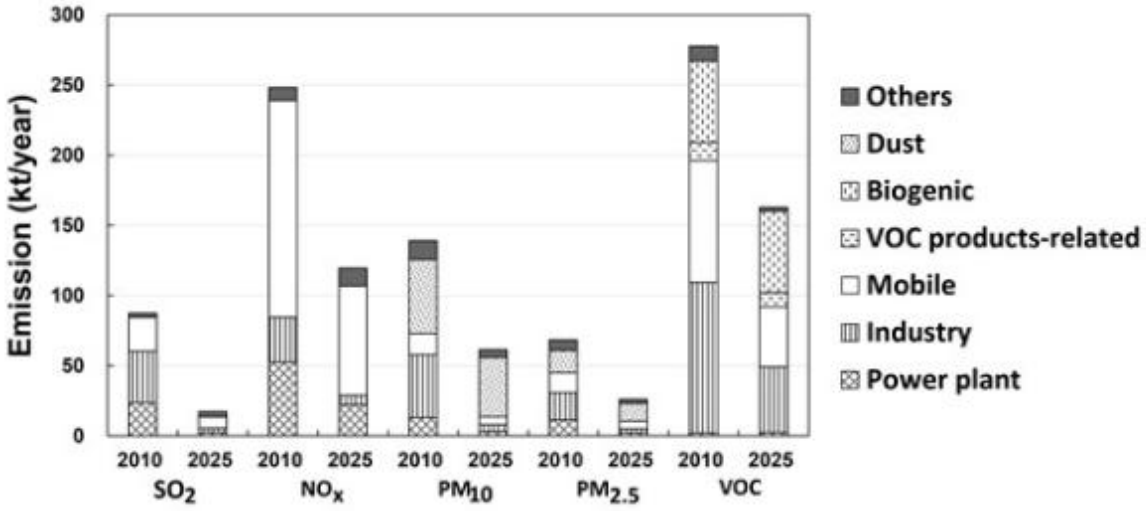

Figure 5 shows total emission amount from each category in Guangzhou in 2010 and 2015.

From Liu et al. (2013), sector-based reduction percentages provide an overview of the control strategy in each sector in the PRD in Figure 6. Power plants, industry and mobile sources are three major contributors for all pollutants reductions, which is similar to Guangzhou. There would be 68%, 43%, 38%, 44% and 29% reduction of SO2, NOx, PM10, PM2.5 and VOCs from these three major sectors in PRD region.

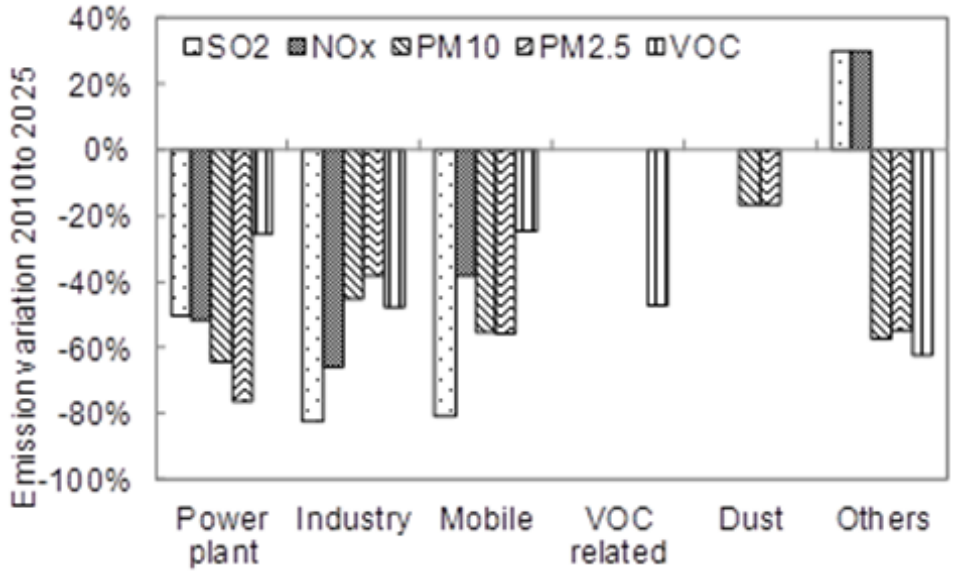

Figure 6 shows sector-based emission reduction percentage in PRD by 2025.

For D1 and D2, the projection of China emissions shall consider (a) No change as of 2020, (b) the emission reduction targets is the same as PRD reduction targets.

4.5 Source Categories

In this study, emission sources are categorized into five major sectors such as power plant, industry, mobile sources, marine emission and area emission. Industry emission sector are treated in two separate ways. For large-scale industry, they are treated as elevated emission, detail information such as the stack height, stack diameter, exit velocity, exit temperature are needed for SMOKE. These parameters are needed to provide for every single stack within the modeling grid. In addition, CMAQ will calculate plume rise for elevated point sources again in CMAQ running. For small-scale industry, they are treated as area emission, and they use population surrogate map to spatially allocate the emission. Power plant sector is treated as elevated point sources while the mobile and other sectors are processed as area sources. Marine emission sector is firstly treated as area sources, and later use a program “Shiplifting” to elevate surface marine emission into high layers. In this study, marine emission is categorized into ocean going vessel and local/river vessel. Ocean goring vessel (OGV) has much high emission amount, and larger stack height compared to local/river vessel (LRV). In our EASEHKPRD system, the marine emissions are categorized as area source in two dimensional space, therefore, the marine emissions only appear in second and third layers, which correspond to 17 m and 35 m above ground, respectively.

5. Chemical Transport Model CMAQ v5.0.1

Community Multi-Scale Air Quality model (CMAQ) is a comprehensive multi pollutant air quality modelling system developed and maintained by the U.S. Environmental Protection Agency's (EPA) Office of Research and Development (ORD). The CMAQ model configuration was the same for all simulations, with the only differences being in the year specific emission and meteorological input data. Aerosols in CMAQ are represented using three lognormal modes: Aitken, accumulation, and coarse (Binkowski and Roselle, 2003). Inorganic species in the Aitken and accumulation modes are assumed to be in thermodynamic equilibrium with the gas phase, while gas-particle partitioning between the gas phase and the coarse mode is treated dynamically. The secondary organic aerosol formulation in CMAQ has been described by Carlton et al. (2010). The simulations in this study used CMAQ version 5.0.1 with the AERO5 aerosol module. (Reff et al., 2009) and source specific ratios of organic mass to organic carbon (Simon and Bhave, 2012). Other CMAQ model options employed include online computation of photolysis rates (Foley et al., 2010), a carbon bond chemical mechanism modified to include chlorine chemistry (CB05CL; Sarwar et al., 2012), and NH3 bi-directional surface exchange (Bash et al., 2012).

Reference

Appel, K.W., Pouliot, G.A., Simon, H., Sarwar, G., Pye, H.O.T., Napelenok, S.L., Akhtar, F., and Roselle, S.J. (2013) Evaluation of dust and trace metal estimates from the Community Multiscale Air Quality (CMAQ) model version 5.0, Geosci. Model Dev., 6, 883-899, doi: 10.5194/gmd-6-883-2013.

Bash, J.O., Cooter, E.J., Dennis, R.L., Walker, J.T., and Pleim, J.E. (2012) Evaluation of a regional air-quality model with bi-directional NH3 exchange coupled to an agro-ecosystem model, Biogeo-sciences Discuss., 9, 11375–11401, doi:10.5194/bgd-9-11375-2012.

Binkowski, F.S., and S.J. Roselle (2003), Models-3 Community Multiscale Air Quality (CMAQ) model aerosol component, 1, Model description, J. Geophys. Res., 108(D6), 4183, doi: 10.1029/2001 JD001409.

Carlton, A.G., P.V. Bhave, S.L. Napelenok, E.D. Edney, G. Sarwar, R.W. Pinder, G.A. Pouliot, and M. Houyoux (2010), Model representation of secondary organic aerosol in CMAQv4.7, Environ. Sci. Technol., 44(22), 8553–8560, doi:10.1021/es100636q.

Foley, K.M., Roselle, S.J., Appel, K.W., Bhave, P.V., Pleim, J.E., Otte, T.L., Mathur, R., Sarwar, G., Young, J.O., Gilliam, R.C., Nolte, C.G., Kelly, J.T., Gilliland, A.B., and Bash, J.O. (2010) Incremental testing of the Community Multiscale Air Quality (CMAQ) modeling system version 4.7, Geosci. Model Dev., 3, 205-226.

Fu, J.S., C.J. Jang, D.G. Streets, Z. Li, R. Kwok, R. Park, and Z. Han (2008), MICS-Asia II: Modeling gaseous pollutants and evaluating an advanced modeling system over East Asia, Atmos. Environ., 42, 3571–3583, doi:10.1016/j.atmosenv.2007.07.058

Fung, J.C.H., A.K.H. Lau, J.S.L. Lam, and Z.B. Yuan (2005) Observational and modeling analysis of a severe air pollution episode in western Hong Kong. J. Geophysical Research – Atmosphere, 110, doi: 10.1029/2004JD005105.

Guenther, A et al. (2006). “Estimates of global terrestrial isoprene emissions using MEGAN (Model of Emissions of Gases and Aerosols from Nature)”. In: Atmospheric Chemistry and Physics 6.1, pp. 3181–3210.

Lam, J.S.L., A.K.H. Lau, and J.C.H. Fung (2006) Application of refined land-use categories for high resolution mesoscale atmospheric modelling. Boundary-Layer Meteorology, 119 (2) 263-288. doi: 10.1007/s10546-005-9027-3.

Li, M et al. (2015). MIX: a mosaic Asian anthropogenic emission inventory for the MICS-Asia and the HTAP projects. Atmospheric Chemistry and Physics Discussions. 2015; 15(23)34813-34869 DOI: 10.5194/ acpd-15-34813-2015

Lo, J.C.F., A.K.H. Lau, J.C.H. Fung, and F. Chen (2006) Investigation of enhanced cross-city transport and trapping of air pollutants by coastal and urban land-sea breeze circulations. J. Geophys. Res., 111, D14104, doi: 10.1029/2005JD006837.

Lo, J.C.F., A.K.H. Lau, F. Chen, J.C.H. Fung, and K.K.M. Leung (2007) Urban modification in a mesoscale model and the effects on the local circulation in the Pearl River Delta region. J. Appl. Meteorol. Climat, 46, 457-476. doi:10.1175/JAM2477.1.

Reff, Adam et al. (2009). Emissions inventory of PM2. 5 trace elements across the United States. In: Environmental science & technology 43.15, pp. 5790–5796.

Sarwar, G., Simon, H., Bhave, P.V., Yarwood, G. (2012) Examining the impact of heterogeneous nitry chloride production on air quality across the United States, Atmos. Phys. Chem., 12,6455-6473.

Simon, H. and Bhave, P.V. (2012) Simulating the degree of oxidation in atmospheric organic particles, Environ. Sci. Technol., 46(1), 331-339, doi:10.1021/es202361w.

Seaman, N.L., D.R. Stauffer and A.M. Lario-Gibbs (1995). A Multiscale Four- Dimensional Data Assimilation System Applied in the San Joaquin Valley during SARMAP. Part I: Modeling Design and Basic Performance Characteristics, J. Appl. Meteorol., 34, 1739–1761.

Stauffer, D.R. and N. L. Seaman, Multiscale four-dimensional data assimilation, J. Appl. Meteor., 33, 416-434, 1994.

Yim, S.H.L., J.C.H. Fung, A.K.H. Lau, and S.C. Kot (2007) Developing a high-resolution wind map for a complex terrain with a coupled MM5/CALMET system. J. Geophys. Res., 112, D05106, doi: 10.1029/2006JD007752.

Yin, Shasha et al. (2015). "A refined 2010-based VOC emission inventory and its improvement on modeling regional ozone in the Pearl River Delta Region, China". In: Science of the Total Environment 514, pp. 426–438.

Zheng, Junyu et al. (2009). "A highly resolved temporal and spatial air pollutant emission inventory for the Pearl River Delta region, China and its uncertainty assessment". In: Atmospheric Environment 43.32, pp. 5112–5122.

Appendix A

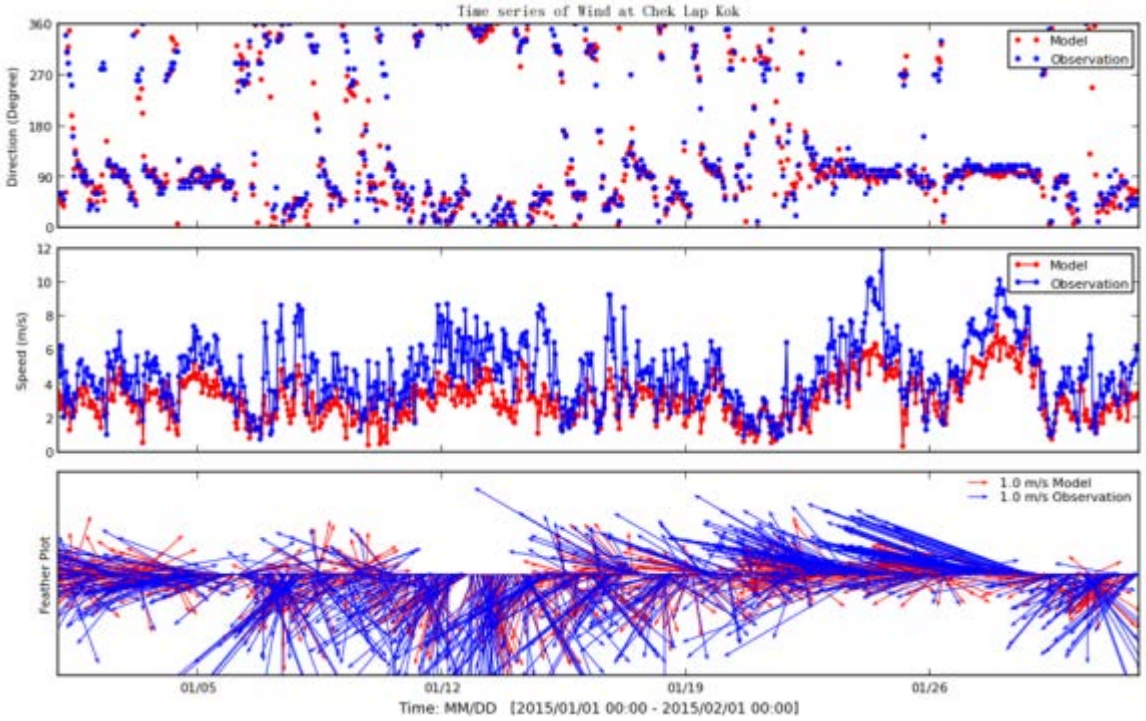

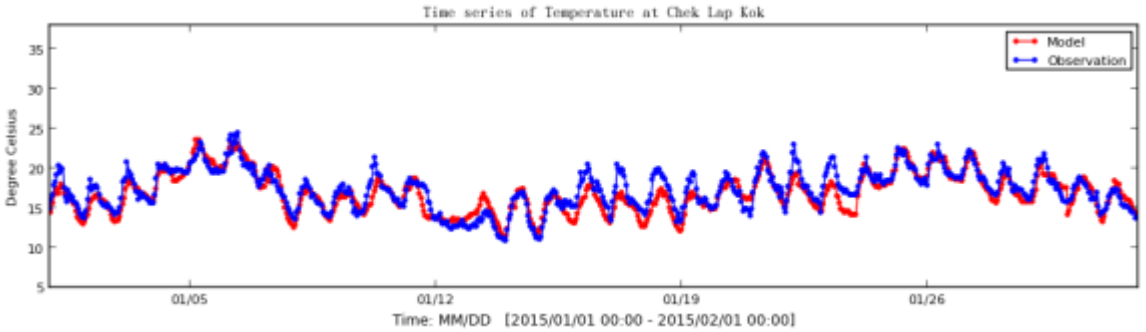

Station Chak Lap Kok

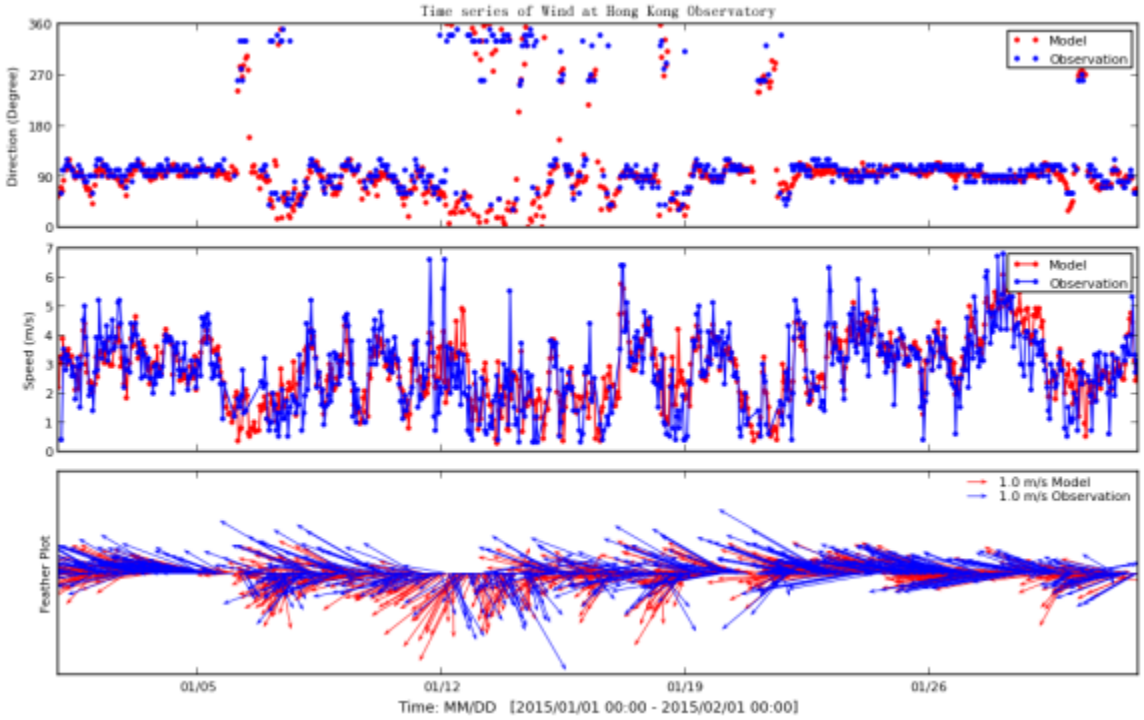

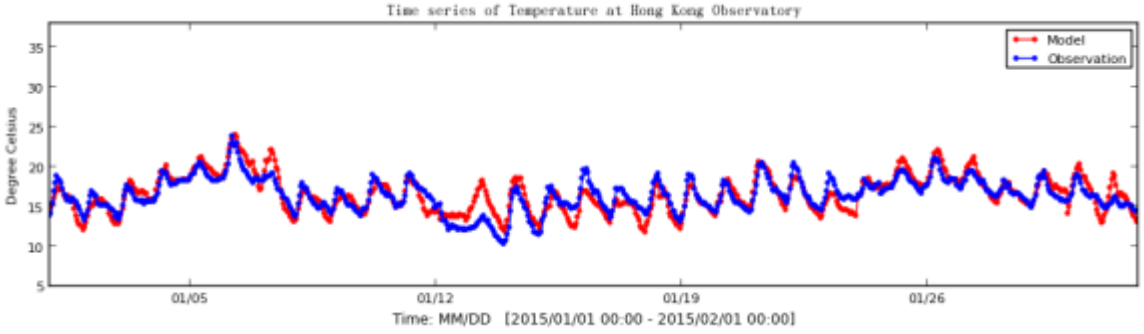

Station HK Observatory

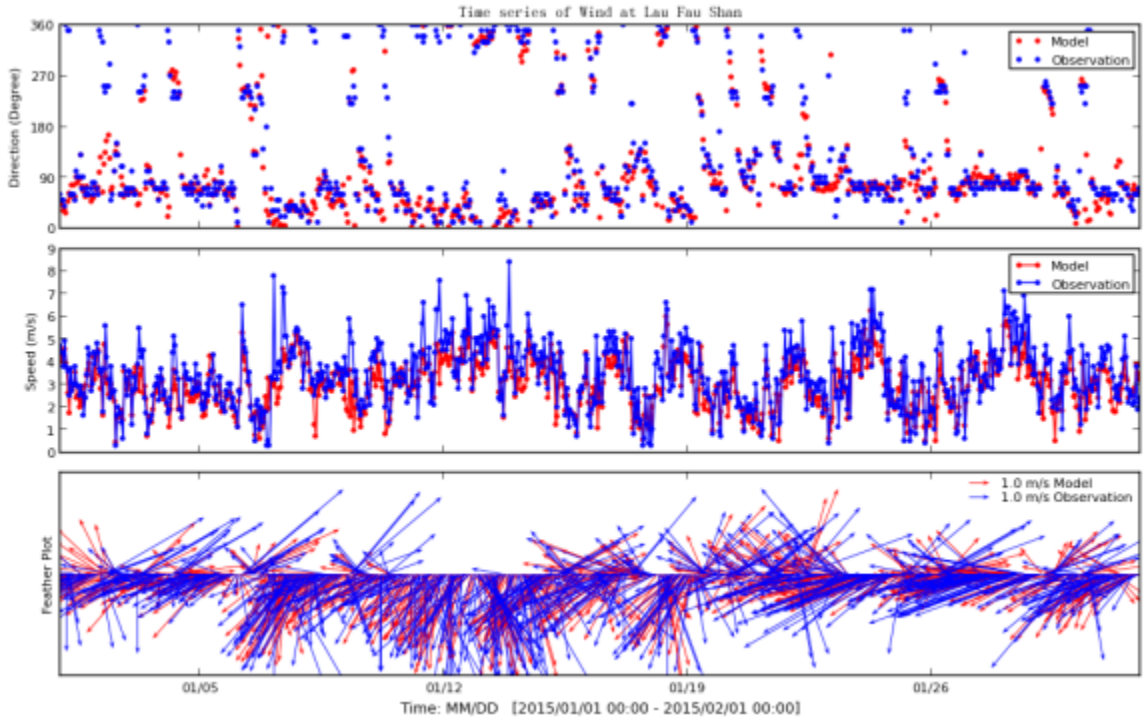

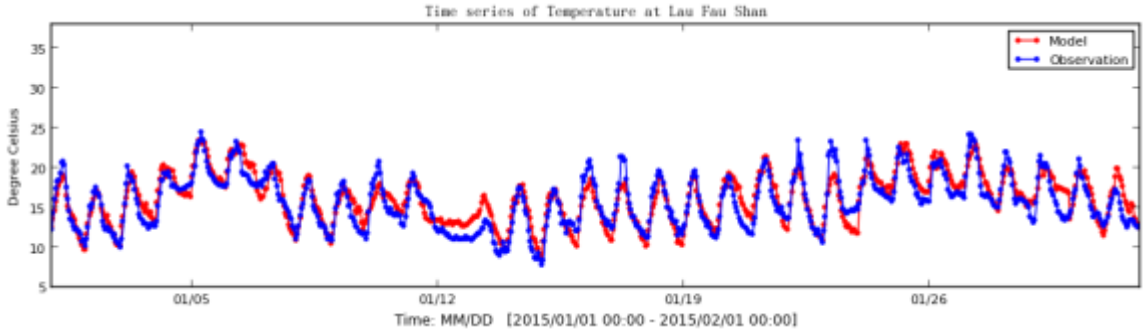

Station Lau Fau Shan

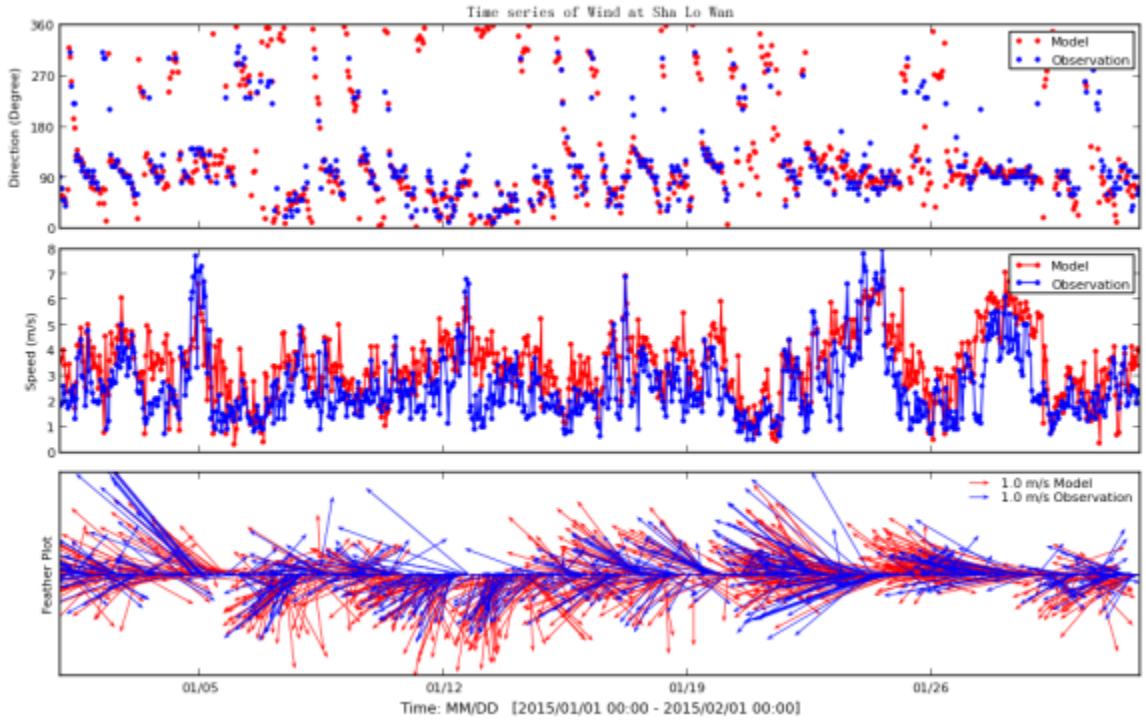

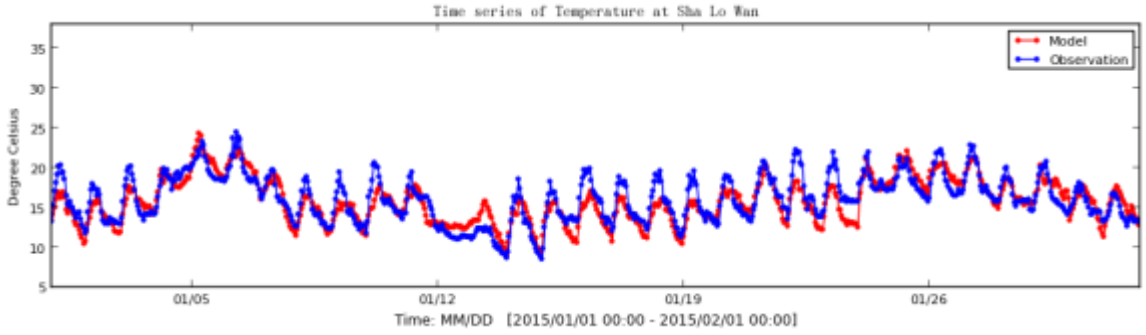

Station Sha Lo Wan

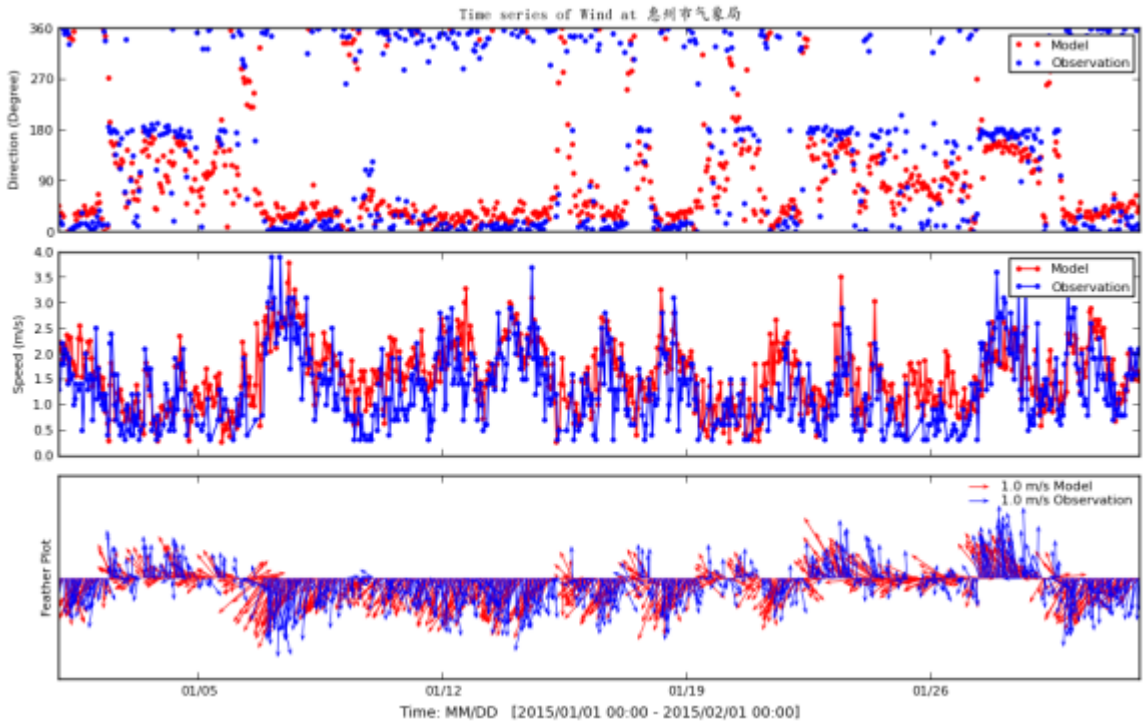

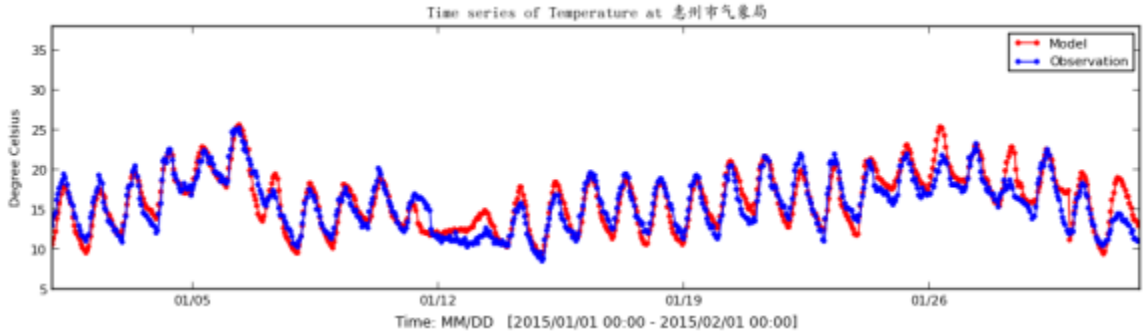

Station: 惠州市气象局

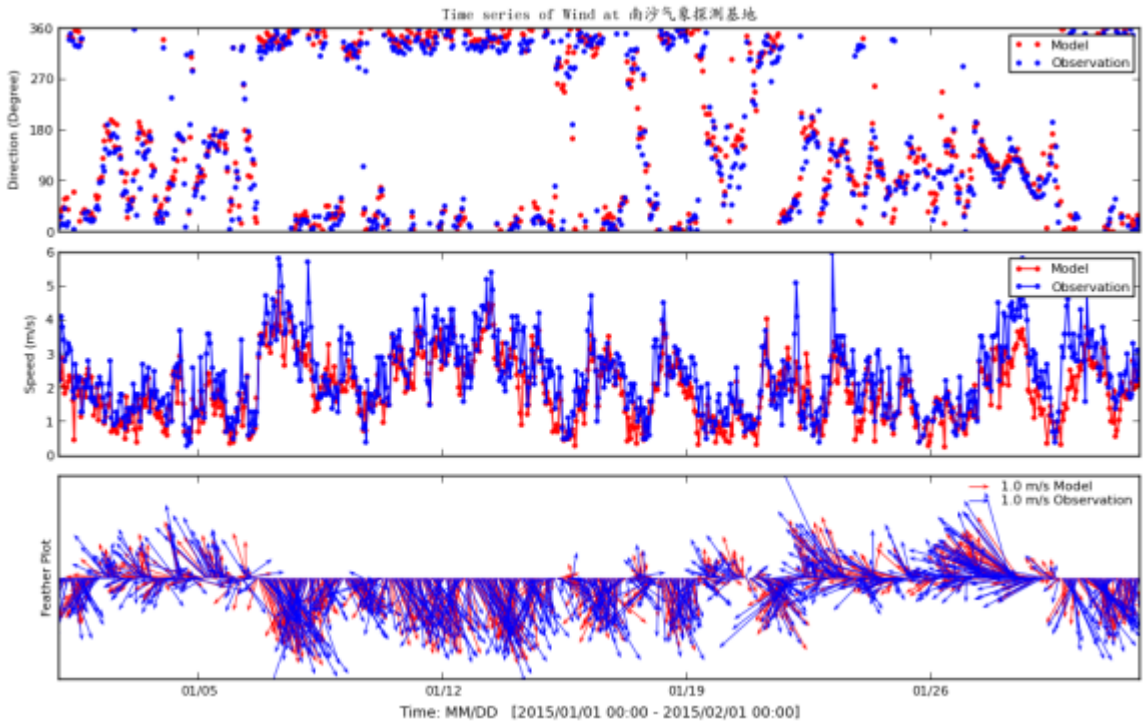

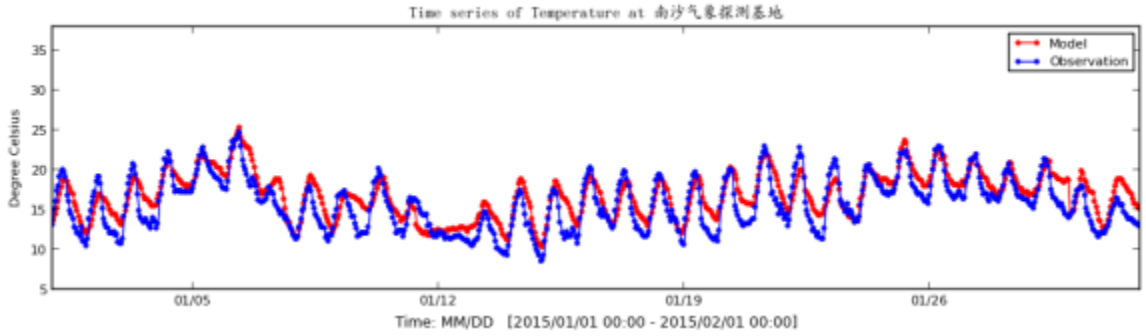

Station: 南沙气象探测基地

Table 1 Statistical Information on Annual (2015) Wind Simulation by WRF

WRF Wind Two way nesting 2015/01/01-2015/12/31																	
Statistical Information:(Wind)																	
Station	1	2	3	4	5	6	7	8	9	10	11	12	13	14	15	16	17
Bluff Head	3.32	2.2	2.04	1.2	0.61	0.48	0.55	5.35	2.98	2.44	1.3	0.74	0.61	0.63	0.59	85.65	0.78
Chek Lap Kok	4.55	0.77	-1.29	-0.23	-0.28	-0.31	0.77	3.27	1.85	1.41	0.3	0.31	0.36	0.75	0.37	196.3	0.51
Chek Lap Kok (2)	4.51	0.98	-0.34	-0.02	-0.07	-0.08	0.77	4.17	1.34	0.95	0.24	0.21	0.24	0.86	0.66	78.82	0.82
Cheung Chau	4.68	1.05	-0.09	0.05	-0.02	-0.01	0.86	4.59	1.23	0.65	0.19	0.14	0.15	0.92	0.6	85.25	0.78
Green Island	5.94	0.91	-1.27	-0.09	-0.21	-0.18	0.78	4.67	2.3	1.55	0.29	0.26	0.29	0.8	0.6	93.95	0.76
Hong Kong Obs	2.55	1.39	0.21	0.39	0.08	0.15	0.79	2.76	0.9	0.68	0.54	0.27	0.33	0.88	0.34	227.2	0.42
Kai Tak	3.17	1.09	0.02	0.09	0.01	0	0.79	3.19	0.98	0.72	0.3	0.23	0.26	0.89	0.38	128.5	0.57
King's Park	2.35	1.34	0.36	0.34	0.16	0.16	0.69	2.72	0.97	0.74	0.49	0.31	0.33	0.81	0.35	199.2	0.46
Lau Fau Shan	3.55	0.94	-0.53	-0.06	-0.15	-0.12	0.78	3.02	1.23	0.81	0.26	0.23	0.26	0.83	0.54	95.78	0.74
Nei Lak Shan	7.79	0.79	-2.82	-0.21	-0.36	-0.36	0.64	4.97	4.27	3.34	0.44	0.43	0.51	0.63	0.27	242	0.42
Ngong Ping	7.03	0.9	-1.95	-0.1	-0.28	-0.26	0.56	5.07	3.66	2.82	0.45	0.4	0.47	0.65	0.25	266	0.4
North Point	3.33	1.18	0.06	0.18	0.02	0.03	0.78	3.4	1.12	0.79	0.38	0.24	0.29	0.88	0.43	185.5	0.49
Ping Chau	1.03	4.25	2.22	3.25	2.16	0.96	0.19	3.25	2.78	2.3	3.3	2.24	1.02	0.26	0.14	183.4	0.43
Sai Kung	2.83	1.23	-0.02	0.23	-0.01	0.06	0.84	2.81	1.04	0.67	0.42	0.24	0.28	0.91	0.42	143.2	0.6
Sha Chau	4.83	1.16	0.11	0.16	0.02	0.05	0.78	4.95	1.53	0.98	0.32	0.2	0.24	0.88	0.34	317.4	0.45
Sha Lo Wan	2.88	1.54	0.82	0.54	0.28	0.29	0.67	3.69	1.56	1.18	0.63	0.41	0.41	0.77	0.41	550.2	0.54
Sha Tin	2.11	1.73	0.86	0.73	0.41	0.35	0.68	2.98	1.41	1.01	0.81	0.48	0.44	0.74	0.2	189.9	0.45
Shek Kong	2.26	1.76	0.5	0.76	0.22	0.26	0.69	2.75	1.22	0.76	0.86	0.34	0.36	0.81	0.26	283.9	0.38
Shell Tsing Yi	2.41	1.39	0.41	0.39	0.17	0.17	0.73	2.82	1.13	0.71	0.51	0.29	0.31	0.83	0.14	195.6	0.41
Siu Ho Wan	3.1	1.42	0.63	0.42	0.2	0.18	0.58	3.73	1.7	1.16	0.58	0.37	0.37	0.74	0.08	423	0.44
Star Ferry - TST	3.57	1.06	-0.42	0.06	-0.12	-0.08	0.79	3.15	1.31	0.9	0.38	0.25	0.31	0.86	0.31	156.6	0.5
Ta Kwu Ling	2	1.48	0.31	0.48	0.16	0.17	0.61	2.31	1.06	0.81	0.69	0.41	0.44	0.77	0.23	163.6	0.48
Tai Mei Tuk	3.24	1.18	-0.06	0.18	-0.02	0.04	0.86	3.18	1.06	0.63	0.34	0.19	0.24	0.92	0.51	117.2	0.64
Tai Mo Shan	7.17	0.95	-2.06	-0.05	-0.29	-0.26	0.58	5.1	3.87	3.01	0.51	0.42	0.5	0.65	0.43	93.29	0.67
Tai Mo To	4.07	1.06	-0.13	0.06	-0.03	-0.02	0.8	3.94	1.24	0.81	0.27	0.2	0.23	0.89	0.29	251.7	0.43
Tai O	5.48	1.08	-0.68	0.08	-0.12	-0.07	0.67	4.8	2.45	1.55	0.38	0.28	0.31	0.78	0.2	293.1	0.41
Tap Mun	2.52	1.35	0.31	0.35	0.12	0.15	0.8	2.83	1.01	0.65	0.48	0.26	0.3	0.89	0.41	137.7	0.65
Tate's Cairn	6.22	0.85	-1.88	-0.15	-0.3	-0.3	0.6	4.34	3.05	2.39	0.42	0.38	0.46	0.65	0.22	131.5	0.51
Tseung Kwan O	1.64	2.13	1.25	1.13	0.76	0.52	0.51	2.89	1.78	1.32	1.17	0.8	0.58	0.52	0.08	302.4	0.39
Tuen Mun	2.42	1.36	0.37	0.36	0.15	0.15	0.75	2.78	0.99	0.69	0.49	0.29	0.31	0.85	0.26	237.1	0.42
Waglan Island	6.2	1.02	-0.3	0.02	-0.05	-0.03	0.9	5.9	1.37	0.74	0.16	0.12	0.13	0.94	0.77	61.01	0.87
Wong Chuk Hang	2.51	1.77	1.01	0.77	0.4	0.34	0.59	3.52	1.71	1.22	0.85	0.49	0.44	0.69	0.17	302.8	0.39
Yi Tung Shan	7.51	0.75	-2.77	-0.25	-0.37	-0.39	0.63	4.74	4.12	3.18	0.41	0.42	0.5	0.63	0.3	268.8	0.42
Average	**3.90**	**1.34**	**-0.16**	**0.34**	**0.10**	**0.06**	**0.70**	**3.75**	**1.82**	**1.32**	**0.58**	**0.39**	**0.37**	**0.77**	**0.35**	**202.65**	**0.53**
Abs Average	**3.90**	**1.34**	**0.85**	**0.41**	**0.26**	**0.21**	**0.70**	**3.75**	**1.82**	**1.32**	**0.58**	**0.39**	**0.37**	**0.77**	**0.35**	**202.65**	**0.53**

Note (1) Observed Wind; (2) Ratio Mean; (3) Mean Bias; (4) Mean Normalized Bias; (5) Norm Mean Bias; (6) Mean Fractionalized Bias; (7) Coefficient Determination; (8) Simulated Mean; (9) Root Mean Square Error; (10) Mean Absolute Gross Error; (11) Mean Normalized Gross Error; (12) Normalized Mean Err; (13) Mean Fractionalized Bias; (14) Index of Agreement. For wind direction: (15) Corr; (16) RMSE and (17) IOA.

Table 2 Statistical Information on annual (2015) Temperature Simulation by WRF

WRF Temperature Two way nesting 2015/01/01-2015/12/31														
Statistical Information:(Temperature)														
Station	**1**	**2**	**3**	**4**	**5**	**6**	**7**	**8**	**9**	**10**	**11**	**12**	**13**	**14**
Chek Lap Kok	25.04	1	-0.12	0	0	0	0.95	24.92	1.66	1.25	0.05	0.05	0.05	0.97
Cheung Chau	23.37	1.02	0.28	0.02	0.01	0.02	0.92	23.65	2.01	1.56	0.07	0.07	0.07	0.95
Hong Kong Obs	24.2	1.02	0.35	0.02	0.01	0.02	0.95	24.54	1.61	1.19	0.05	0.05	0.05	0.97
Kat O	21.91	1.02	0.3	0.02	0.01	0.01	0.89	22.21	2.33	1.68	0.08	0.08	0.08	0.94
King's Park	23.75	1.04	0.81	0.04	0.03	0.04	0.95	24.56	1.81	1.34	0.06	0.06	0.06	0.97
Lau Fau Shan	23.79	1.03	0.57	0.03	0.02	0.03	0.94	24.36	2	1.46	0.07	0.06	0.07	0.96
Nei Lak Shan	18.36	1.1	1.41	0.1	0.08	0.08	0.95	19.77	2.19	1.73	0.11	0.09	0.1	0.95
Ngong Ping	20.01	1.11	1.98	0.11	0.1	0.1	0.94	21.99	2.57	2.14	0.12	0.11	0.11	0.93
Pak Tam Chung	22.74	1.04	0.42	0.04	0.02	0.03	0.93	23.16	2.23	1.77	0.09	0.08	0.09	0.96
Ping Chau	23.66	1.02	0.41	0.02	0.02	0.02	0.92	24.07	2.04	1.56	0.07	0.07	0.07	0.96
Sai Kung	23.62	1.04	0.74	0.04	0.03	0.03	0.95	24.36	1.83	1.39	0.07	0.06	0.06	0.97
Sha Lo Wan	23.86	1.01	0.07	0.01	0	0.01	0.94	23.93	1.85	1.36	0.06	0.06	0.06	0.97
Sha Tin	23.8	1.01	0.15	0.01	0.01	0.01	0.94	23.95	1.86	1.41	0.07	0.06	0.07	0.97
Shek Kong	23.93	1.03	0.43	0.03	0.02	0.02	0.94	24.36	2.01	1.5	0.07	0.06	0.07	0.97
Ta Kwu Ling	23.39	1.04	0.71	0.04	0.03	0.04	0.94	24.09	2.11	1.57	0.08	0.07	0.07	0.97
Tai Mei Tuk	23.8	1	-0.17	0	-0.01	0	0.93	23.63	2.11	1.61	0.07	0.07	0.07	0.96
Tai Mo Shan	17.7	1.1	1.48	0.1	0.08	0.09	0.95	19.17	2.11	1.71	0.12	0.1	0.11	0.95
Tai Po	23.55	1.03	0.54	0.03	0.02	0.03	0.94	24.09	1.92	1.45	0.07	0.06	0.07	0.97
Tap Mun	22	1.07	1.34	0.07	0.06	0.06	0.94	23.34	2.31	1.79	0.09	0.08	0.09	0.96
Tate's Cairn	19.87	1.09	1.4	0.09	0.07	0.08	0.95	21.27	2.24	1.77	0.1	0.09	0.1	0.96
The Peak	20.76	1.05	0.88	0.05	0.04	0.04	0.95	21.63	1.72	1.31	0.07	0.06	0.07	0.97
Tseung Kwan O	23.41	1.02	0.32	0.02	0.01	0.02	0.94	23.73	1.87	1.45	0.07	0.06	0.07	0.97
Tsing Yi	24.47	1.03	0.59	0.03	0.02	0.03	0.95	25.06	1.74	1.25	0.06	0.05	0.05	0.97
Tuen Mun	24.55	1.03	0.49	0.03	0.02	0.02	0.94	25.04	1.87	1.4	0.06	0.06	0.06	0.97
Tuen Mun Child.	24.1	0.99	-0.46	-0.01	-0.02	-0.02	0.94	23.65	1.92	1.52	0.07	0.06	0.07	0.97
Waglan Island	23.51	1.01	0.11	0.01	0	0.01	0.93	23.62	1.92	1.45	0.07	0.06	0.07	0.96
Wong Chuk Hang	24.04	0.97	-0.83	-0.03	-0.03	-0.04	0.95	23.22	1.79	1.46	0.07	0.06	0.07	0.97
Average	**22.86**	**1.03**	**0.53**	**0.03**	**0.02**	**0.03**	**0.94**	**23.38**	**1.99**	**1.52**	**0.08**	**0.07**	**0.07**	**0.96**
Abs Average	**22.86**	**1.03**	**0.64**	**0.04**	**0.03**	**0.03**	**0.94**	**23.38**	**1.99**	**1.52**	**0.08**	**0.07**	**0.07**	**0.96**

Note (1) Observed Wind; (2) Ratio Mean; (3) Mean Bias; (4) Mean Normalized Bias; (5) Norm Mean Bias; (6) Mean Fractionalized Bias; (7) Coefficient Determination; (8) Simulated Mean; (9) Root Mean Square Error; (10) Mean Absolute Gross Error; (11) Mean Normalized Gross Error; (12) Normalized Mean Err; (13) Mean Fractionalized Bias; (14) Index of Agreement.

Appendix B

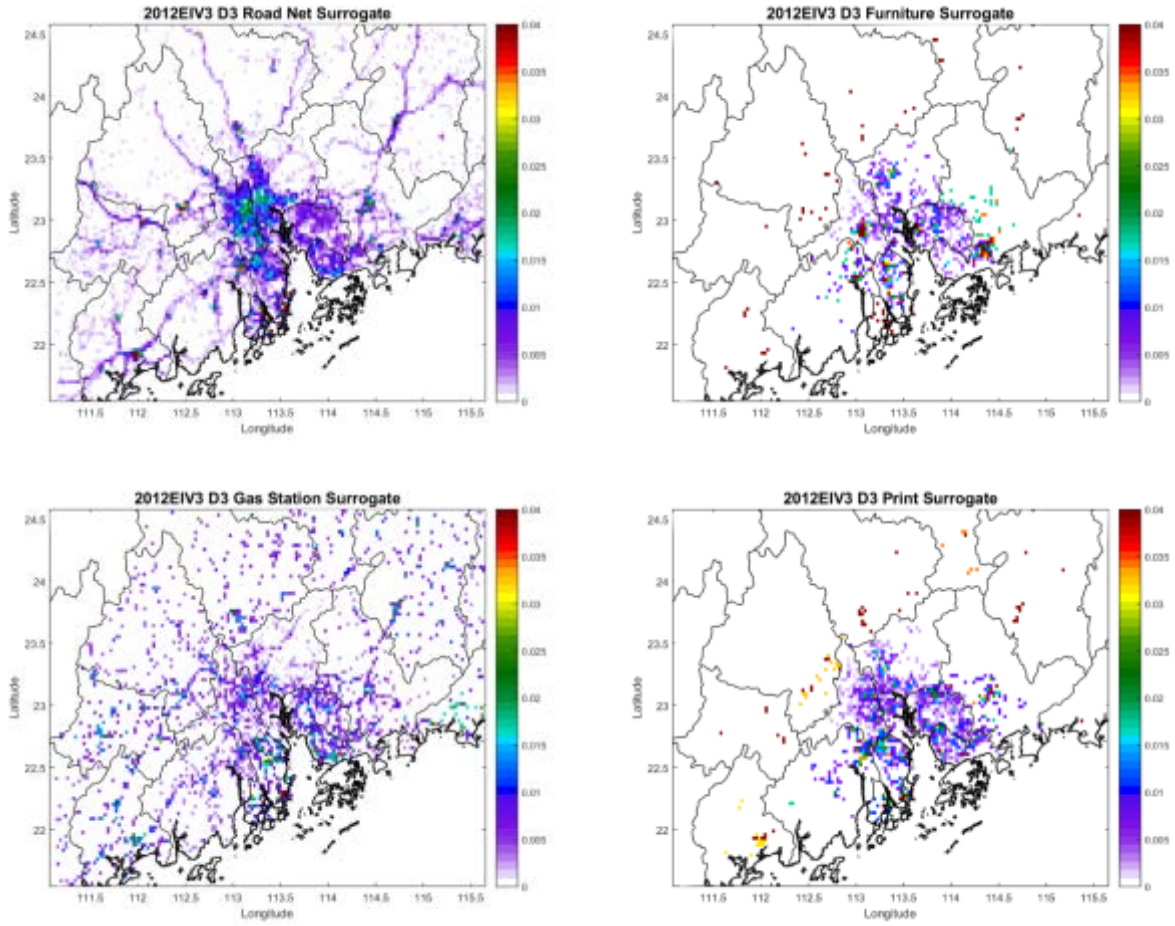

Figure B1. Example of spatial surrogate map for road network, furniture, gas stations and print shops in D3 with 3km resolution.

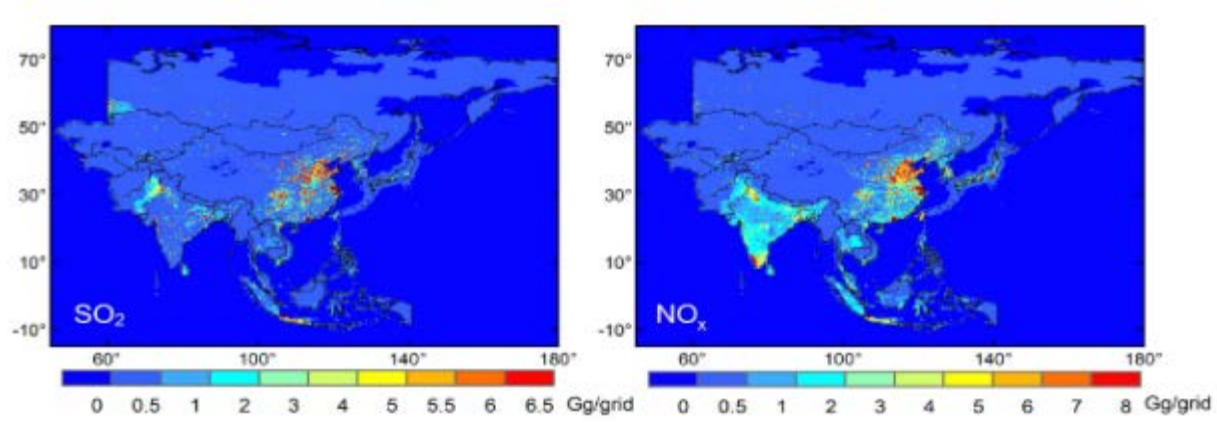

Figure B2. Example of MIX dataset from Tsinghau University.

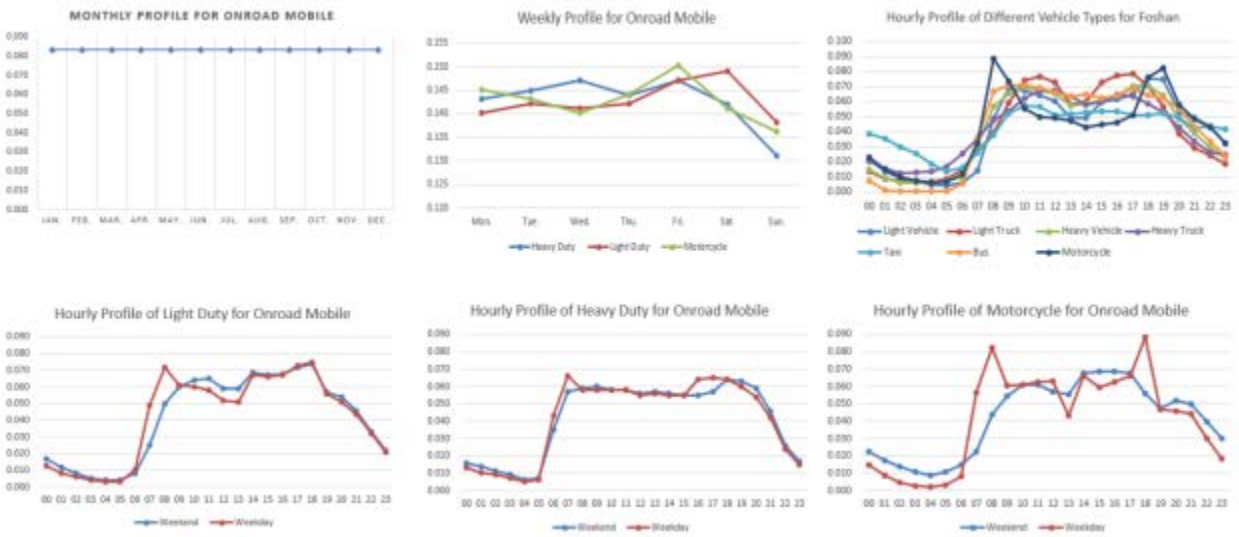

Figure B3. Example of temporal profiles for on-road mobile.

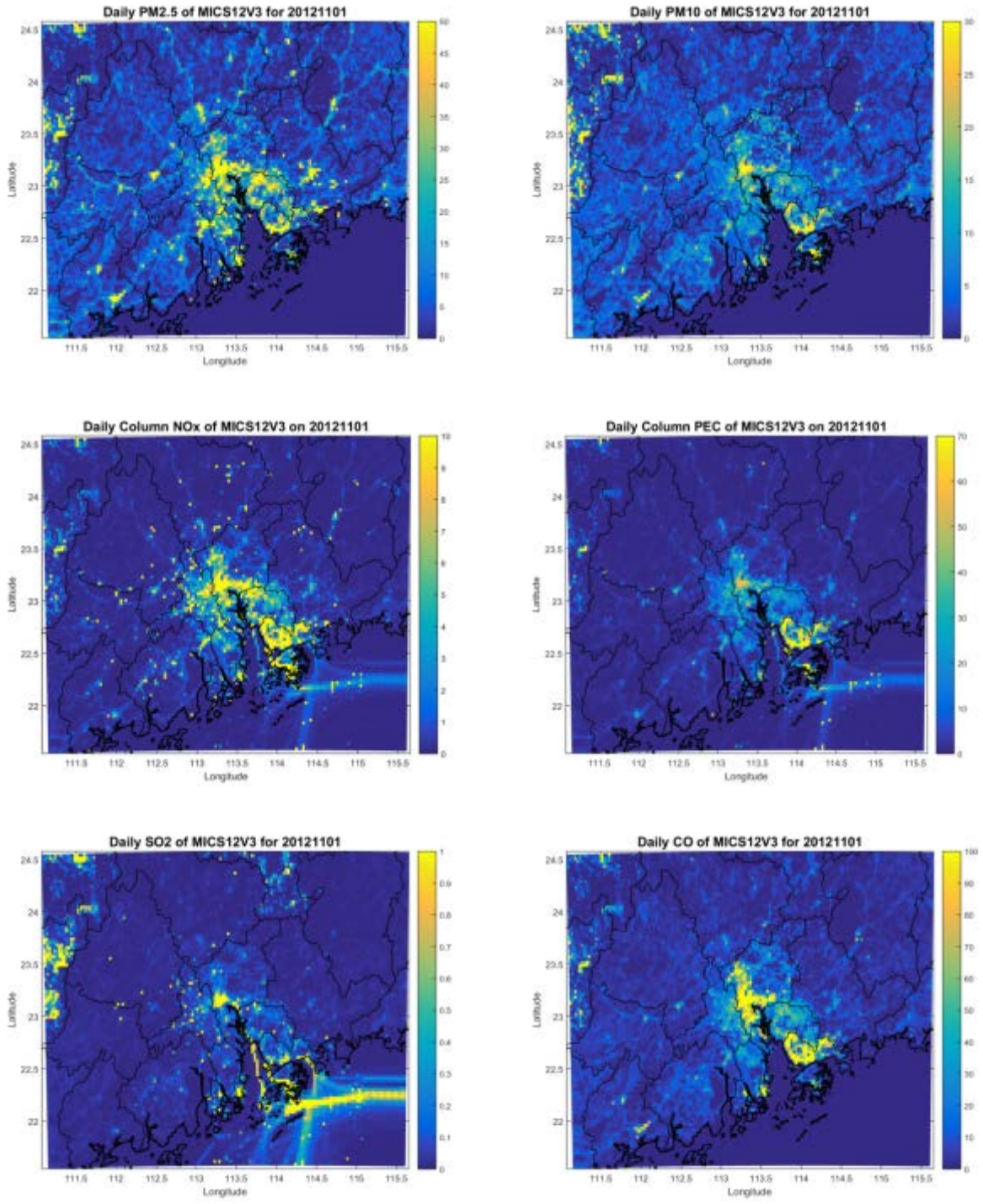

Figure B4. Example of model ready emission for PM2.5, PM10, NOx, PEC, SO2 and CO for D3 with 3km resolution.

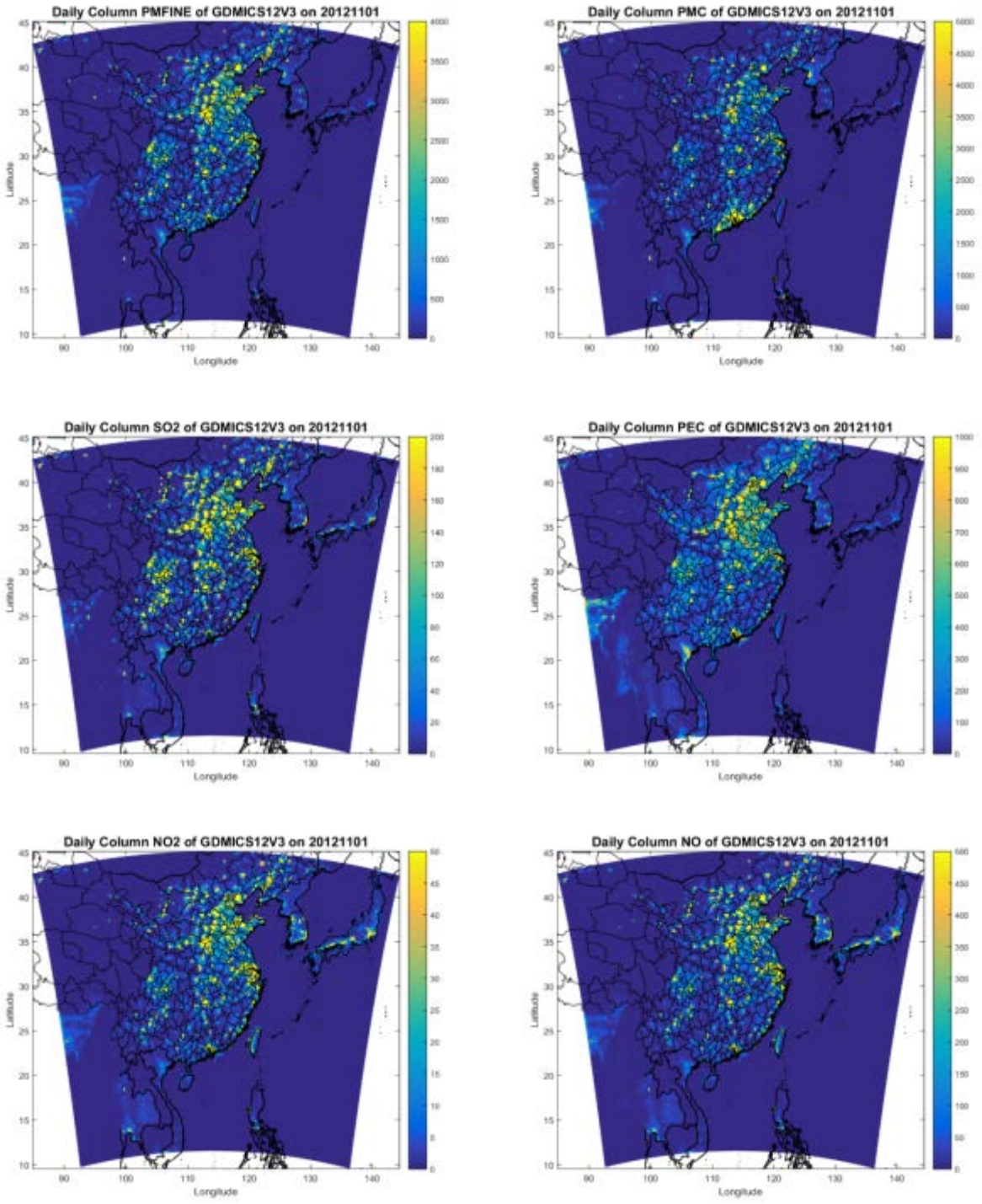

Figure B5. Example of model ready emission for PM2.5, PM10, SO2, PEC, NO2 and NO for D1 with 27km resolution.